Ordering of water molecules between phospholipid bilayers visualized by coherent anti-Stokes Raman scattering microscopy

Ji-Xin Cheng*†, Sophie Pautot‡§, David A. Weitz‡, and X. Sunney Xie*¶

Departments of *Chemistry and Chemical Biology and ‡Physics and Division of Engineering and Applied Sciences, Harvard University, Cambridge, MA 02138

Edited by Robin M. Hochstrasser, University of Pennsylvania, Philadelphia, PA, and approved June 23, 2003 (received for review April 15, 2003)

We demonstrate ordered orientation of the hydration water at the surface of phospholipid bilayers by use of coherent anti-Stokes Raman scattering (CARS) microscopy, a highly sensitive vibrational imaging method recently developed. We investigated negatively charged POPS (1-palmitoyl-2-oleoyl-sn-glycero-3-phospho-L-serine) and neutral POPC (1-palmitoyl-2-oleoyl-sn-glycero-3-phosphocholine) multilamellar onions dispersed in deuterated dodecane. The imaging contrast based on the CARS signal from the H_2O stretching vibration shows a clear dependence on the excitation field polarization. Our results provide direct experimental evidence that water molecules close to the phospholipid bilayer surface are ordered with the symmetry axis along the direction normal to the bilayer. Moreover, the amount of ordered water molecules depends on the lipid polar group. The spectral profile for the interlamellar water shows that the water molecules bound to the bilayer surface are less hydrogen-bonded and exhibit a higher vibrational frequency than bulk water.

Membranes formed by bilayers of phospholipids play a pervasive and central role in many cellular functions. Whenever two such membranes come in contact, short-range interactions between the membranes are critical for a multitude of processes. These interactions are mainly hydration forces resulting from partial orientation of interlamellar water by the bilayer (1) and steric repulsions resulting from contact between lipid molecules in the opposing bilayers (2, 3). Hydration forces (4) have been identified as the dominant nonspecific short-range interactions that account for the repulsive pressure between two lipid bilayers when their separation is in the range of 1.0 to 3.0 nm (1, 5). Several models have been developed that relate the hydration force with the ordering of water molecules on a membrane surface (6–8). Molecular dynamics (MD) simulation studies (9, 10) have suggested that water is partially ordered within 1.0 nm from the membrane surface. However, experimental results have supplied only partial information regarding the exact nature of liquid water organization in the vicinity of bilayers. Some evidence for water bound to a membrane surface was provided by [^{2}H]NMR studies, in which the quadrupolar splitting frequency of deuterated water was found to decrease with increasing hydration level (11, 12). In addition, Fourier transform infrared (FTIR) studies (13) supported by a recent MD simulation (14) have shown that water molecules are hydrogen-bonded to the oxygen atoms of the PO_2^- group in the phospholipid polar head moiety and the ester C=O group of the sn-2 acyl chain. In principle, the net orientation of the interfacial water molecules at a membrane surface can be probed by polarization measurements. In fact, such an attempt has been made in a sum frequency generation study of water/lipid monolayer interface (15). However, ordering of water was not observed for the particular sample used. To the best of our knowledge, no direct experimental evidence for ordering of water on a membrane surface in relation with the membrane hydration has been reported to date.

In this paper, we report a multiphoton vibrational imaging study of onion-like structures that consist of multiple alternate layers of phospholipid and water. We use coherent anti-Stokes Raman scattering (CARS) microscopy (16, 17) in which a pump laser beam at frequency ω_p and a Stokes laser beam at frequency ω_s are tightly focused into a sample to generate an anti-Stokes signal at frequency $2\omega_p - \omega_s$. CARS microscopy allows 3D vibrational imaging with high sensitivity. The vibrational contrast arises from the enhancement of the CARS signal when $\omega_p - \omega_s$ is tuned to a Raman band (18). The 3D sectioning ability results from the nonlinear dependence of CARS signals on the excitation field intensity, similar to two-photon fluorescence microscopy (19). The high-sensitivity is a consequence of the constructive addition of CARS signal from an ensemble of vibrational oscillators in the excitation volume.

The multilamellar onions dispersed in deuterated dodecane, prepared via a self-emulsification process (20), provide an ideal system for investigating the properties of water between lipid bilayers. The water molecules in this preparation are present only between the bilayers for these onions. The use of a fully deuterated oil solvent allows selective imaging of lipids based on the vibrational signal from the C—H stretching mode, and of the interlamellar water based on the vibrational signal from the O—H stretching mode. The coherent addition of the CARS fields from multiple layers of water molecules produces a strong CARS signal, which allows us to study the properties of water confined between contacting lipid bilayers.

In particular, the relation between the excitation field polarization and the Raman tensor α allows us to characterize the orientation of a symmetric molecule such as H_2O or a symmetric functional group such as CH_2. With the pump and Stokes beams polarized parallel along or perpendicular to the symmetry axis, the CARS signal arises from the α_{11} or α_{22} components (1 and 2 are the directions parallel and perpendicular to the molecular symmetry axis), respectively (21). Because α_{22}/α_{11} is much less than 1, the contrast should depend strongly on the excitation polarization for molecules with ordered orientation. Combining the polarization sensitivity and the vibrational specificity of CARS microscopy, we image individual onions to obtain a direct visual confirmation of the water orientation, as well as evidence for the correlation of the water orientation with that of the lipid. We also provide evidence that the ordering degree of water decreases with increasing interlamellar separation and that water—water hydrogen bonding is weakened for the water molecules bound to the lipid bilayer.

This paper was submitted directly (Track II) to the PNAS office.

Abbreviations: CARS, coherent anti-Stokes Raman scattering; POPS, 1-palmitoyl-2-oleoyl-*sn*-glycero-3-phospho-L-serine; POPC, 1-palmitoyl-2-oleoyl-*sn*-glycero-3-phosphocholine.

†Present address: Department of Biomedical Engineering, Purdue University, 500 Central Drive, West Lafayette, IN 47907.

§Present address: Lawrence Berkeley National Laboratory, Material Science Division, Berkeley, CA 94720.

¶To whom correspondence should be addressed at: Department of Chemistry and Chemical Biology, Harvard University, 12 Oxford Street, Cambridge, MA 02138. E-mail: xie@chemistry.harvard.edu.

www.pnas.org/cgi/doi/10.1073/pnas.1732202100

Materials and Methods

Sample Preparation. POPS (1-palmitoyl-2-oleoyl-*sn*-glycero-3-phospho-L-serine) and POPC (1-palmitoyl-2-oleoyl-*sn*-glycero-3-phosphocholine) were purchased from Avanti Polar Lipids. A dried lipid film was dissolved in fully deuterated dodecane (Cambridge Isotope Laboratories, Cambridge, MA) at a concentration of 0.25 mg/ml. When a water droplet was injected into the solution at controlled temperature, lipids assembled at the oil-water interface to form a multilamellar film. As water diffused between the bilayers, the film swelled and led to the spontaneous formation of onions in the oil phase with a diameter of several micrometers as well as smaller emulsion droplets. The size was determined by the initial lipid concentration and the temperature; once the onions formed, they remained insensitive to temperature changes (20). After a few hours, a small volume of the dodecane suspension was collected and placed between two coverslips for imaging studies.

Method. The vibrational imaging experiments were carried out by using a laser-scanning CARS microscope that acquires a frame of 512 × 512 pixels in several seconds with a lateral resolution of 0.23 μm and an axial resolution of 0.75 μm. Details of the CARS microscope have been described elsewhere (22). The pump and Stokes beams were from two near infrared 5-ps (spectral width 2.9 cm^{-1}) pulse trains synchronized to an 80-MHz clock (23). All images were acquired at 21°C.

Results and Discussion

Orientation of Phospholipids and Interlamellar Water. The lateral CARS images of two POPS multilamellar vesicles with the laser beams focused into the equatorial plane are displayed in Fig. 1. By tuning $\omega_p - \omega_s$ to 2,845 cm^{-1}, the CARS peak for the symmetric CH_2 stretching vibration (24), we observed a strong contrast from the lipid molecules, as shown in Fig. 1 *A* and *B*. Moreover, the contrast was bipolar and maximized along the *y* direction when *x*-polarized pump and Stokes beams were used (Fig. 1*A*). When the polarization of both beams was rotated by 90° from the *x* to the *y* direction, the contrast was rotated by 90° (Fig. 1*B*). The CARS signal from the symmetric CH_2-stretching mode is maximized when the excitation polarization is along the CH_2 group symmetry axis that is perpendicular to the lipid hydrocarbon chain (Fig. 2). Thus, our observation is consistent with the ordered orientation of the lipid hydrocarbon chains within a bilayer (25).

To image the interlamellar water that is distributed around the lipid polar head (26), we tuned $\omega_p - \omega_s$ into the broad OH-stretching Raman band at 3,445 cm^{-1}. Under the same excitation condition, the maximum direction of the water contrast (Fig. 1 *C* and *D*) is perpendicular to that of the CH_2 contrast (Fig. 1 *A* and *B*). The main contribution to the resonant CARS signal from condensed phase water in the OH-stretching vibration region is the symmetric mode (ν_1), similar to the Raman signal (27). Therefore, the CARS images in Fig. 1 demonstrate that the interlamellar water molecules are strongly ordered, with their symmetry axis along the lipid hydrocarbon chain, as depicted in Fig. 2. The orientated water molecules contribute to a positive electrostatic potential inside the membrane, which compensates the negative potential from the lipid polar head (11, 28).

Dependence on Interlamellar Spacing. To explore the dependence of the ordering on the thickness of the water layer, we varied the sample preparation temperature. It is known that the amount of interlamellar water increases with preparation temperature (29). CARS images of POPS onions prepared at 15, 25, and 40°C are shown in Fig. 3 *A*, *B*, and *C*, respectively. All of the images were

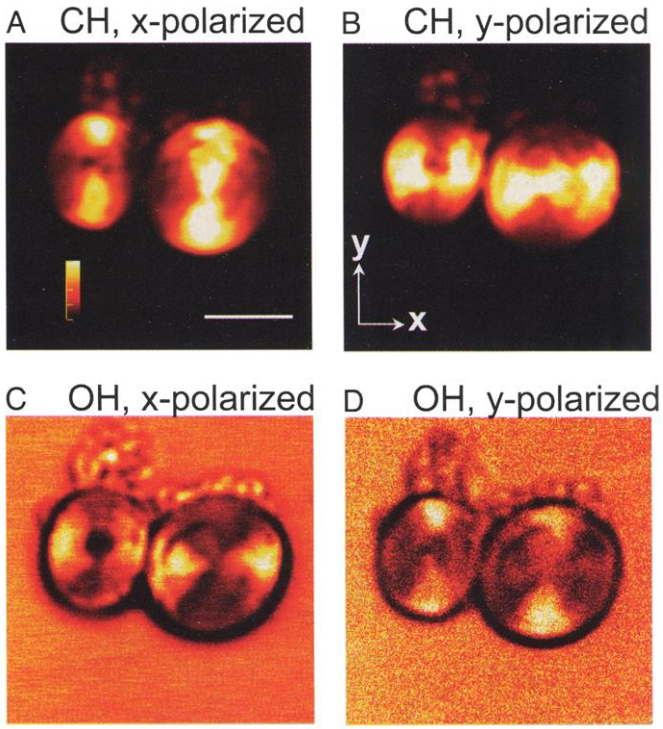

Fig. 1. CARS images of POPS multilamellar onions prepared at 27°C. $\omega_p - \omega_s$ was tuned to 2,845 cm^{-1} (*A* and *B*) and 3,445 cm^{-1} (*C* and *D*). (Scale bar, 5 μm.) The number of bilayers was estimated to be ≈500. Each image of 250 × 250 pixels was acquired at a dwell time of 10 μs per pixel, and the final image was an average of five scans. The polarization direction of the parallel-polarized pump and Stokes beams is marked above each image. The pump frequency was fixed at 14,212 cm^{-1}. The average powers of the pump and the Stokes beam were 100 and 50 mW, respectively, at a repetition rate of 80 MHz. The onion core is composed of deuterated dodecane based on the CARS images (not shown) with $\omega_p - \omega_s$ tuned to the CD-stretching vibration at 2,125 cm^{-1}.

acquired at 21°C. The pump and the Stokes beams were parallel-polarized with $\omega_p - \omega_s$ tuned to the O—H-stretching vibration. The water contrast along the *x* direction and that along the *y* direction are characterized by the ratio of the maximum CARS intensity of the onions along the *x* direction (I_x^{max}) and that along the *y* direction (I_y^{max}) to the nonresonant background from the deuterated dodecane oil solvent (I_{sol}), respectively (Fig. 3 *D* and *E*). I_x^{max} is the sum of the nonresonant background from the lipid and the resonant signal from the ordered and the isotropic water. I_y^{max} is the sum of the nonresonant background from lipid and the resonant signal from the isotropic water because the ordered water contributes little to the CARS signal along the *y* direction. Fig. 3 *D* and *E* suggests that the amount of the interlamellar water of the POPS onions increases as the preparation temperature increases from 15–25°C and then saturates for higher temperatures.

To evaluate the percentage of oriented water molecules in the interlamellar space, we compare the difference of the CARS intensities along the *x* and the *y* directions. Fig. 3*F* shows that I_x^{max}/I_y^{max} drops with the preparation temperature, indicating that the percentage of ordered water molecules decreases with increasing interlamellar water amount (larger interlamellar space). At low interlamellar separation, a majority of the water molecules are ordered whereas, at larger interlamellar separation, a significant amount of the interlamellar water behaves as bulk water. The dependence of the percentage of ordered water on the interlamellar space is in agreement with molecular dynamics simulation results showing that polarization of water

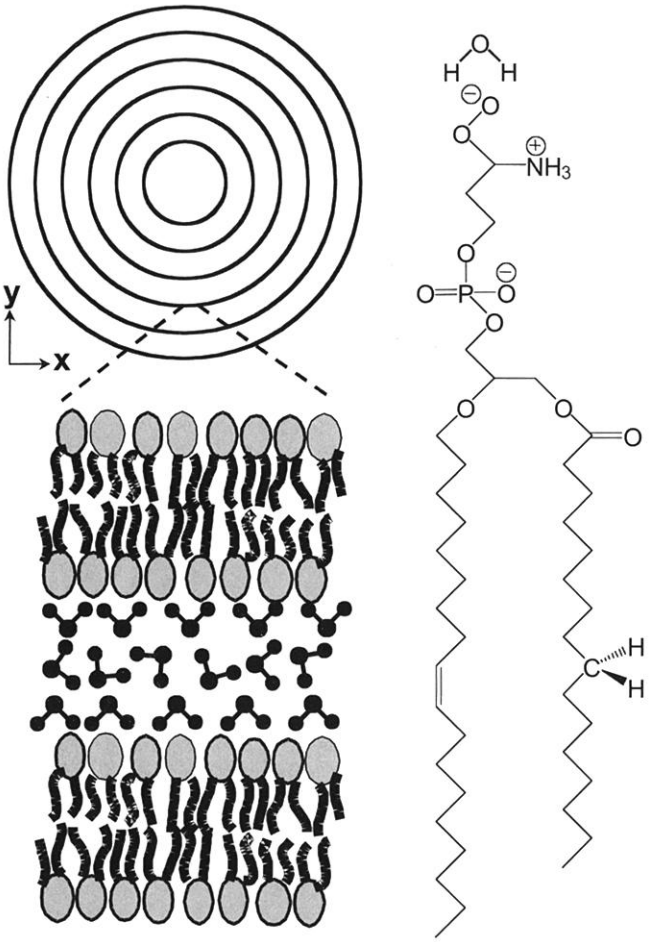

Fig. 2. (*Left*) Schematic of a multilamellar vesicle in an equatorial plane and the orientation of interlamellar water. (*Right*) The configuration of a POPS molecule with a water molecule on the polar head. Orientation of the water molecule and the CH_2 groups in the hydrocarbon chain is illustrated.

molecules occurs only within 1.0 nm of the membrane/water interface (10). As the interlamellar space increases, the repulsive hydration forces between bilayers decrease (1, 5), which is confirmed by the decrease of the onion size indicating that the pressure difference inside and outside the onion emulsion increases.

Spectral Profiles of POPS Lipid and Interlamellar Water. To explore the nature of the interactions between water and lipids that leads to the ordering of the water molecules bound to the membrane surface, we acquired a series of CARS images of an identical POPS onion prepared at 27°C in a broad Raman shift range from 3,748 to 2,746 cm^{-1}. The results using *x*-polarized excitation fields are shown in Fig. 4*A*. In the entire OH-stretching vibration region from 3,748 to 3,117 cm^{-1}, the water contrast was maximized along the *x* direction. When $\omega_p - \omega_s$ was tuned to the C—H-stretching vibration region from 2,990 to 2,846 cm^{-1}, the contrast was maximized along the *y* direction (compare Fig. 1). This finding confirms that the main contribution to the CARS signal arises from the CH_2 symmetric stretching mode (24). When $\omega_p - \omega_s$ was tuned to 2,800 and 2,746 cm^{-1}, away from any Raman resonance, the polarization dependence disappeared.

The contrast for the interlamellar water was calculated as the maximum CARS intensity along the *x* direction from the onion

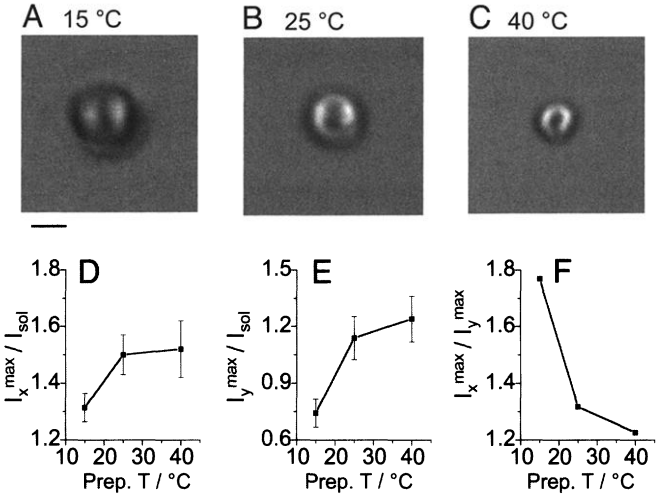

Fig. 3. (*A–C*) CARS images of POPS onions prepared at 15, 25, and 40°C, respectively. (Scale bar, 2 μm.) Each image recorded at 21°C consists of 200 × 200 pixels. The pump beam at frequency 14,209 cm^{-1} and the Stokes beam at frequency 10,760 cm^{-1} were parallel-polarized along the *x* direction. The other acquisition parameters were the same as in Fig. 1. (*D*) Dependence of the water contrast along the *x* direction, I_x^{max}/I_{sol}, on the preparation temperature. (*E*) Dependence of the water contrast along the *y* direction, I_y^{max}/I_{sol}, on the preparation temperature. (*F*) Dependence of I_x^{max}/I_y^{max} on the preparation temperature. I_x^{max} and I_y^{max} are the maximum CARS intensities from the onion along the *x* and *y* directions, respectively. I_{sol} is the CARS intensity from the dodecane solvent. The fluctuation of the contrast amplitude between different onions prepared under the same temperature was ≈10%.

normalized by the CARS intensity from the oil solvent. The wavelength dependence is plotted in Fig. 4*B*. For comparison, we also report the CARS and spontaneous Raman spectra of bulk liquid water recorded at 21°C. The CARS spectrum of bulk water is shifted toward lower wavenumbers as a consequence of the interference between the resonant and the nonresonant contributions (18), and the CARS spectral profile differs from the Raman profile because of the interference between adjacent vibrational bands (30). The spectral profile for the interlamellar water contains both the resonant contributions from water and the nonresonant background, which is frequency independent. In contrast to bulk water, the CARS spectral profile for the interlamellar water extends to the higher wavenumber region. Based on the effect of the hydrogen bonding on the OH-stretching vibrational frequency (31), we conclude that the hydrogen bonding for these water molecules bound to the bilayer surface is reduced. A similar weakening of hydrogen bonding was reported for water interacting with hydrophobic surfaces of CCl_4 and hexane (32).

Using the same CARS images in Fig. 4*A*, the spectral profile for the POPS lipid was calculated as the maximum CARS intensity along the *y* direction from the onion normalized by the CARS intensity from the oil solvent and is plotted in Fig. 4*C*. Apparently, the contrast for the POPS lipid is much higher than that for the interlamellar water because of a much higher density of C—H bonds in the onion. The dip around 3,050 cm^{-1}, which explains the negative contrast in the image at 3,016 cm^{-1}, arises from the destructive interference between the nonresonant background and the resonant signal from the lipid. Comparing the spectral profile in Fig. 4*C* and the multiplex CARS spectrum of DOPC (1,2-dioleoyl-*sn*-glycero-3-phosphocholine) (24), we found that POPS, with a phase transition temperature of 14°C, was in the liquid crystalline phase for these onions prepared at 27°C.

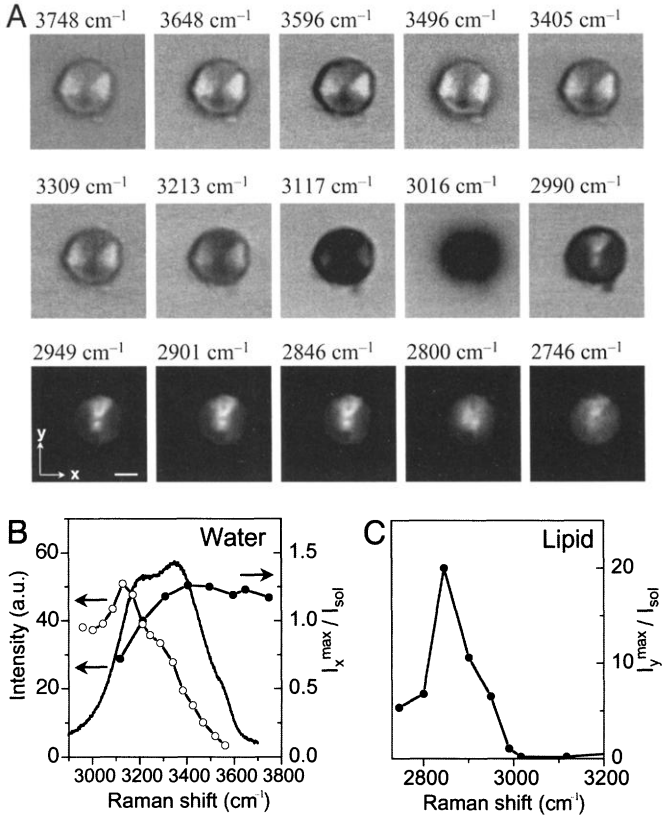

Fig. 4. (A) CARS images of identical POPS vesicles prepared at 27°C at different Raman shifts marked above each image. Each image consists of 210 × 210 pixels. (Scale bar, 2 μm.) The pump laser frequency was fixed at 14,395 cm^{-1}. The average powers of the *x*-polarized pump and Stokes beams were 100 and 50 mW, respectively. In the C—H-stretching vibration region, a lower photon multiplier tube voltage was used to avoid the saturation of the strong CARS signal from the lipid, which resulted in lower background intensities for the images in the third row than in the first two rows. (*B*) Wavelength dependence of the CARS contrast for the interlamellar water (filled circles plus line). The CARS (open circles plus line) and the spontaneous Raman (line) spectra of bulk water are also shown. The CARS spectrum of bulk water was acquired on a Nikon microscope with the pump frequency fixed at 14,395 cm^{-1}. The CARS signal was recorded with a single photon avalanche diode and was normalized by the Stokes power and the transmission rate of the bandpass filter at each Raman shift. The spontaneous Raman spectrum of pure liquid water was recorded on a Raman microspectrograph (LabRam, Jobin-Yvon, Longjumeau, France) with an 1,800-groves/mm grating and a 15-mW HeNe laser at 632.8 nm. (*C*) Wavelength dependence of the CARS contrast for the POPS lipid.

Dependence on Lipid Polar Head Groups. To investigate the effect of the lipid polar head group on the orientation of the water molecules, similar imaging experiments were performed with multilamellar onions formed with POPC, a zwitterionic phospholipid. We observed the same dependence on the excitation polarization as in Fig. 1, and thus the same ordering of the water molecules with respect to the lipid bilayer. Comparing the CARS intensities, we found that, when prepared at 15°C, the interlamellar space of the POPC onions contains fewer water molecules than that of the POPS onions. This finding is consistent with the fact that the repulsion between the zwitterionic POPC bilayers is lower than the charged POPS bilayers. Moreover, the percentage of ordered molecules for POPC onions is found to be lower than for POPS onions prepared under the same condition, which we attribute to the stronger hydrogen bonding of interfacial water with the negatively charged carboxylate moiety in the POPS head group. For water-saturated onions prepared at 40°C, the water contrast (I_x^{max}/I_{oil} = 1.9) for POPC onions is larger than that (1.5) observed for POPS onions, indicating a larger interlamellar space between POPC bilayers than between POPS bilayers. Moreover, the value of I_x^{max}/I_y^{max} is 1.5 for the POPC and 1.2 for the POPS onions. This result suggests that the ordering of water observed at the saturation level results mainly from the dipole potential of the lipid head group (28) and that POPS has a less negative dipole potential than POPC because of the serine group.

Conclusions

In summary, our CARS imaging study of multilamellar phospholipid onions provides experimental evidence that water molecules close to the bilayer surface are strongly ordered, with their dipoles aligned against the bilayer dipole (Fig. 2), and that the percentage of oriented molecules decreases with an increase in the interlamellar spacing. Our observations are consistent with the presence of a hydration force between two lipid bilayers. Furthermore, the spectral profile of the CARS contrast for the interlamellar water shows a weakening of the hydrogen bonding for the water molecules bound to the lipid bilayer.

Although molecular orientation at interfaces has been extensively studied by second-harmonic generation and sum-frequency generation spectroscopy (33, 34), our results show that CARS microscopy provides a powerful means for chemically selective imaging. It allows us to determine distribution as well as orientation of specific molecules or functional groups with 3D spatial resolution. Moreover, the spectral profiles provide us with information regarding the nature of molecular interactions. Based on the single membrane sensitivity of CARS microscopy (22, 35), the present work can potentially be extended to investigate the role of water in the interaction between two biological membrane surfaces, such as occurs during membrane and vesicle fusion (36).

This work was supported by the National Science Foundation through the Harvard Materials Research Science and Engineering Center (DMR-0213805).

1. Leikin, S., Parsegian, V. A., Rau, D. C. & Rand, R. P. (1993) *Annu. Rev. Phys. Chem.* **44,** 369–395.
2. Israelachvili, J. N. & Wennerstrom, H. (1992) *J. Phys. Chem.* **96,** 520–531.
3. Harbich, W. & Helfrich, W. (1984) *Chem. Phys. Lipids* **36,** 39–63.
4. LeNeveu, D. M., Rand, R. P. & Parsegian, V. A. (1976) *Nature* **259,** 601–603.
5. McIntosh, T. J. & Simon, S. A. (1994) *Annu. Rev. Biophys. Biomol. Struct.* **23,** 27–51.
6. Marcelja, S. & Radic, N. (1976) *Chem. Phys. Lett.* **42,** 129–130.
7. Attard, P. & Batchelor, M. T. (1988) *Chem. Phys. Lett.* **149,** 206–211.
8. Kornyshev, A. A. & Leikin, S. (1989) *Phys. Rev. A* **40,** 6431–6437.
9. Saiz, L. & Klein, M. L. (2002) *Acc. Chem. Res.* **35,** 482–489.
10. Marrink, S.-J. & Berkowitz, M. (1995) in *Permeability and Stability of Lipid Bilayers*, eds. Disalvo, E. A. & Simon, S. A. (CRC, Boca Raton, FL).
11. Gawrisch, K., Ruston, D., Zimmerberg, J., Parsegian, V. A., Rand, R. P. & Fuller, N. (1992) *Biophys. J.* **61,** 1213–1223.
12. König, S., Sackmann, E., Richter, D., Zorn, R., Carlile, C. & Bayerl, T. M. (1994) *J. Chem. Phys.* **100,** 3307–3316.
13. Wong, P. T. T. & Mantsch, H. H. (1988) *Chem. Phys. Lipids* **46,** 213–224.
14. Pasenkiewicz-Gierula, M., Takaoka, Y., Miyagawa, H., Kitamura, K. & Kusumi, A. (1997) *J. Phys. Chem. A* **101,** 3677–3691.
15. Walker, R. A., Gragson, D. E. & Richmond, G. L. (1999) *Colloids Surf. A* **154,** 175–185.
16. Zumbusch, A., Holtom, G. R. & Xie, X. S. (1999) *Phys. Rev. Lett.* **82,** 4142–4145.
17. Cheng, J. X., Volkmer, A. & Xie, X. S. (2002) *J. Opt. Soc. Am. B* **19,** 1363–1375.
18. Shen, Y. R. (1984) *The Principles of Nonlinear Optics* (Wiley, New York).
19. Denk, W., Strickler, J. H. & Webb, W. W. (1990) *Science* **248,** 73–76.
20. Pautot, S., Frisken, B. J., Cheng, J. X., Xie, X. S. & Weitz, D. A. (2003) *Langmuir*, in press.

21. Levenson, M. D. & Kano, S. S. (1988) *Introduction to Nonlinear Laser Spectroscopy* (Academic, San Diego).
22. Cheng, J. X., Jia, Y. K., Zheng, G. & Xie, X. S. (2002) *Biophys. J.* **83,** 502–509.
23. Cheng, J. X., Volkmer, A., Book, L. D. & Xie, X. S. (2001) *J. Phys. Chem. B* **105,** 1277–1280.
24. Cheng, J. X., Volkmer, A., Book, L. D. & Xie, X. S. (2002) *J. Phys. Chem.* **106,** 8493–8498.
25. Nagle, J. F. & Tristram-Nagle, S. (2000) *Curr. Opin. Struct. Biol.* **10,** 474–480.
26. Wiener, M. C. & White, S. H. (1992) *Biophys. J.* **61,** 434–447.
27. Carey, D. M. & Korenowski, G. M. (1998) *J. Chem. Phys.* **108,** 2669–2675.
28. Simon, S. A. & McIntosh, T. J. (1989) *Proc. Natl. Acad. Sci. USA* **86,** 9263–9267.
29. Marsh, D. (1990) *CRC Handbook of Lipid Bilayers* (CRC, Boca Raton, FL).
30. Maeda, S., Kamisuki, T. & Adachi, Y. (1988) in *Advances in Non-linear Spectroscopy*, eds. Clark, R. J. H. & Hester, R. E. (Wiley, New York), p. 253.
31. Scherer, J. R. (1978) in *Advances in Infrared and Raman Spectroscopy*, eds. Clark, R. J. H. & Hester, R. E. (Wiley, New York).
32. Scatena, L. F., Brown, M. G. & Richmond, G. L. (2001) *Science* **292,** 908–912.
33. Shen, Y. R. (1989) *Annu. Rev. Phys. Chem.* **40,** 327–350.
34. Eisenthal, K. B. (1996) *Chem. Rev.* **96,** 1343–1360.
35. Potma, E. O. & Xie, X. S. (2003) *J. Raman Spectrosc.*, in press.
36. Prestegard, J. H. & O'Brien, M. P. (1987) *Annu. Rev. Phys. Chem.* **38,** 383–411.